Defective Acidification in Human Breast Tumor Cells and Implications for Chemotherapy

By Nihal Altan,* Yu Chen,* Melvin Schindler,‡ and Sanford M. Simon*

*From the *Laboratory of Cellular Biophysics, Rockefeller University, New York 10021; and the*
‡*Department of Biochemistry, Michigan State University, East Lansing, Michigan 48824*

Summary

Multidrug resistance (MDR) is a significant problem in the treatment of cancer. Chemotherapeutic drugs distribute through the cyto- and nucleoplasm of drug-sensitive cells but are excluded from the nucleus in drug-resistant cells, concentrating in cytoplasmic organelles. Weak base chemotherapeutic drugs (e.g., anthracyclines and vinca alkaloids) should concentrate in acidic organelles. This report presents a quantification of the pH for identified compartments of the MCF-7 human breast tumor cell line and demonstrates that (*a*) the chemotherapeutic Adriamycin concentrates in acidified organelles of drug-resistant but not drug-sensitive cells; (*b*) the lysosomes and recycling endosomes are not acidified in drug-sensitive cells; (*c*) the cytosol of drug-sensitive cells is 0.4 pH units more acidic than the cytosol of resistant cells; and (*d*) disrupting the acidification of the organelles of resistant cells with monensin, bafilomycin A1, or concanamycin A is sufficient to change the Adriamycin distribution to that found in drug-sensitive cells, rendering the cell vulnerable once again to chemotherapy. These results suggest that acidification of organelles is causally related to drug resistance and is consistent with the hypothesis that sequestration of drugs in acidic organelles and subsequent extrusion from the cell through the secretory pathways contribute to chemotherapeutic resistance.

Key words: multidrug resistance • pH • secretion • chemotherapy • breast cancer

Successful chemotherapy requires that tumor cells be more sensitive to chemotherapeutic agents than normal cells of the body. However, a major impediment to such treatment of cancer is the development of resistance by the tumor not only to the drugs administered but also to a host of other structurally and mechanistically diverse drugs to which the tumor has not been exposed (1). This phenomenon has been termed multidrug resistance (MDR).[1]

Research during the past 20 years has discovered many genetic differences between drug-resistant and drug-sensitive tumor cells (2). These include changes in the type and amount of cellular lipids and in the expression of proteins, including P-glycoprotein (Pgp) (3, 4), MDR-associated protein (MRP) (5), glutathione *S*-transferase (6), protein kinase C (7), DNA topoisomerase II (8), and the vacuolar proton ATPase (9). In addition to these genetic differences, there are dramatic differences in the intracellular concentration and distribution of chemotherapeutic drugs. In drug-sensitive cells, chemotherapeutic drugs are diffuse throughout the cytoplasm and nucleus. In contrast, in drug-resistant cells, chemotherapeutic drugs accumulate only within discrete cytoplasmic organelles; almost none is detectable in the nucleus (10–14).

Many chemotherapeutic drugs, such as the anthracyclines and vinca alkaloids, are weak bases with pK_a values between 7.4 and 8.4 (15, 16). They are membrane permeable in their neutral form and relatively membrane impermeant when protonated (17). When these drugs diffuse into acidified liposomes or acidified red blood cell ghosts, they become protonated, thus membrane impermeable, and sequestered (17–20). Likewise, upon entering any of the acidic compartments of the cell (such as the lysosome, recycling endosomes, *trans*-Golgi network [TGN], or secretory vesicles), it is predicted that they will become protonated and sequestered within these compartments. Based on these observations, the protonation, sequestration, and secretion (PSS) model has been proposed to account for the relative sensitivity of tumor cells and resistance of MDR cells to weak base chemotherapeutic drugs (21). The PSS hypothesis postulates that acidified organelles (in MDR and nontransformed cells) protonate chemotherapeutic drugs, thereby sequestering them from the nucleoplasm and cytosol (the aqueous phase of the cytoplasmic compartment). The drugs are subsequently secreted from

---

[1]*Abbreviations used in this paper:* LAMP, lysosome-associated membrane protein; MDR, multidrug resistance; MRP, MDR-associated protein; Pgp, P-glycoprotein; PSS, protonation, sequestration, and secretion; SNARF, seminaphthorhodafluor; TGN, *trans*-Golgi network.

the cell through the normal pathways of vesicular traffic and secretion. The model proposes that the enhanced sensitivity of tumor cells to chemotherapeutic drugs is a consequence of a reduced acidification within these organelles and, thus, a reduced ability to sequester the drugs away from the cytosol and nucleoplasm. The PSS hypothesis makes the following four predictions: (*a*) chemotherapeutic drugs should accumulate within the acidic secretory organelles of drug-resistant cells; (*b*) there should be a significant quantitative difference between drug-sensitive and MDR tumor cells in either the organellar acidification or transport; (*c*) agents that disrupt organellar acidification should reverse drug resistance; and (*d*) agents that reverse drug resistance should either block acidification or block secretion from acidified organelles.

There have been several studies measuring the total cellular pH of drug-resistant and drug-sensitive tumor-derived cell lines, with differing results that suggest greater acidification in drug-sensitive cells (22–25). In a previous study, we reported that the drug-sensitive MCF-7 human breast tumor cell line lacks highly acidified organelles (21). Similar results have been reported in the K-562 erythroblastoma leukemia cells (26). However, studies have not been done quantifying the pH in identified compartments of the cell.

In this report, we quantify the pH in identified cellular compartments, including the cytosol, the nucleus, the recycling endosomes, and the lysosomes of both MCF-7 and MCF-7/ADR drug-resistant cell lines. Further, we identify the organelles in MDR-7/ADR drug-resistant cells which accumulate adriamycin. These results demonstrate that in MCF-7/ADR cells, adriamycin accumulates in the acidic compartments of the cell, e.g., the lysosomes, TGN, and recycling endosomes. The pH profile of the MCF-7/ADR cells was similar to nontransformed cells (27–29): the cytosolic pH was neutral, and the lysosomes and endosomes were acidified. However, in striking contrast, the cytosol of the MCF-7 cells was considerably more acidic, and the lumen of the lysosomes and recycling endosomes was considerably more alkaline. As a result, the organelles of MCF-7 cells had substantially reduced transmembrane pH gradients. Disrupting the pH gradients in the MCF-7/ADR cells to resemble the pH in the MCF-7 cells dissipated the chemotherapeutic drugs from the acidified organelles and reversed drug resistance.

Materials and Methods

Bodipy-transferrin, LysoSensor Blue DND-167, FITC-transferrin, seminaphthorhodafluor (SNARF)-dextran, NBD-ceramide, and FITC-dextran were from Molecular Probes, Inc. (Eugene, OR). Adriamycin was from Calbiochem Corp. (San Diego, CA). Concanamycin A was from Fluka Chemical Corp. (Buchs, Switzerland). Bovine insulin and l-glutamine were from GIBCO BRL (Gaithersburg, MD), and FBS was from Gemini Bio-Products, Inc. (Calabasas, CA). The anti–lysosome-associated membrane protein (LAMP) 1 serum was from the Developmental Hybridoma Bank at Johns Hopkins University (Baltimore, MD), and goat anti–mouse secondary antibody Fab fragments conjugated to

phycoerythrin were from Jackson ImmunoResearch Laboratories, Inc. (West Grove, PA). All other reagents were from Sigma Chemical Co. (St. Louis, MO).

Tissue Culture

MCF-7 and MCF-7/ADR cells were obtained from Dr. William Wells of the Department of Biochemistry, Michigan State University. They were maintained in Modified Eagle's medium with phenol red, bovine insulin 10 μg/ml, l-glutamine, and 10% FBS in a humidified incubator at 37°C and 5% CO_2 (Forma Scientific, Inc., Marietta, OH). In addition, the MCF-7/ADR cells were maintained continuously in 0.8 μM Adriamycin. The MCF-10F cells were obtained from American Type Culture Collection (Rockville, MD).

Cell Imaging

All incubations were at 37°C with 5% CO_2. Unless otherwise stated, the cells were incubated in DME without phenol red or serum and with 20 mM Hepes, pH 7.3. All incubation and imaging was at 37°C in coverglass chambers (Lab-tek, Naperville, IL) with media preequilibrated with 5% CO_2, and the chamber was superfused with humified air containing 5% CO_2.

Confocal Microscopy. Unless specifically stated, all imaging measurements were performed on an Ultima confocal microscope (Meridian Instruments, Inc., Okemos, MI) equipped with an argon laser. Cells were visualized with a 60×/1.4NA oil objective (Olympus Optical Co., Ltd., Tokyo, Japan), and the data were collected with two photomultiplier tubes (R3896; Hamamatsu Photonics, Hamamatsu City, Japan).

Epifluorescence Microscopy. A fluorescence microscope (Diaphot; Nikon, Inc., Melville, NY) was used for pH measurements within the lumens of recycling endosomes. The microscope was equipped with a 100 W Hg lamp and Uniblitz shutter (Vincent and Associates, Rochester, NY). The shuttering of the light source was controlled with a computer. The data were collected on an intensified charged coupled device (4910; Hamamatsu Photonics).

Adriamycin Labeling. Adriamycin is a small heterocyclic amine (molecular mass 580 dalton) with a pK_a of 8.3 that can diffuse across membranes in the uncharged form. Adriamycin fluorescence is excited between 350 and 550 nm and emits between 400 and 700 nm. Cells were incubated with Adriamycin (10 μM) for 30 min at 37°C and then visualized using the confocal microscope with (λ_{ex} = 488 nm).

Acridine Orange Labeling. Cells were incubated with acridine orange (6 μM) for 15 min and then visualized on the confocal microscope (λ_{ex} = 488 nm). Emission light passed through a 560-nM short-pass dichroic mirror. The green emission passed through a 530/30-nm bandpass filter, and the red emission passed through a 610-nm longpass filter. The green and red emissions were collected using two photomultiplier tubes.

Lysosome Labeling. Cells were incubated with LysoSensor Blue DND-167 (2 μM, 1 mM stock in water) for 60 min, and then visualized on the confocal microscope (λ_{ex} = 353 nm). In some experiments, the cells were subsequently washed and incubated with Adriamycin (10 μM) for 30 min.

TGN Labeling with NBD-ceramide. Cells were incubated in DME/20 mM Hepes, pH 7.3, with NBD-ceramide (5 μM) at 4°C for 10 min (30). They were then washed twice with DME/20 mM Hepes (pH 7.3)/10% FBS, incubated at 37°C for 30 min, and observed with the confocal microscope (λ_{ex} = 488 nm).

BODIPY-transferrin Labeling of the Recycling Endosome Compartment. BODIPY-transferrin was used to label the recycling endosome compartment. Transferrin is endocytosed by specific receptors on the surface of the cell, then transported through the endosomes and recycled back to the surface. The transferrin receptor is not transported to the lysosomes, so probes that are conjugated to transferrin can be used to selectively monitor the recycling endocytic compartments (31). The endocytic pathway is known to undergo acidification (32). Thus, the fluorophore BODIPY was used, since its fluorescence is not very sensitive to pH. The cells were loaded with 50 μg/ml of BODIPY-transferrin in DME/20 mM Hepes, pH 7.3, for 25 min in a humidified incubator at 37°C and 5% CO_2 (31). The cells were washed rapidly three times with DME/Hepes, incubated for 2 min in a citric acid buffer, pH 4, at 37°C, and rinsed three times with HBSS containing 20 mM Hepes, pH 7.3. In some experiments, the cells were subsequently incubated at 37°C for 30 min to allow the transferrin to recycle to the surface, and then incubated with Adriamycin (10 μM) at 37°C for 30 min.

pH Measurements

The pH-sensitive fluorophores, FITC and SNARF, were used to measure the pH within endosomes and the cytosol, respectively. LysoSensor Blue DND-167 was also used as an independent probe for calibration of the pH within the lumenal compartment of lysosomes. Both FITC and SNARF are ratiometric dyes. The emission intensity of FITC at 530 nm increases with increasing pH at λ_{ex} = 490 nm. However, it is unaffected by pH at λ_{ex} = 450 nm. Therefore, by taking the ratio of the emission intensities at the two excitation wavelengths, one can obtain a pH value independent of FITC concentration in a particular compartment. To convert the ratios to pH values, the cells were calibrated using monensin and nigericin with buffers of known pH (see below). FITC is most useful for measurement of pH values of 5.0–7.0.

SNARF at λ_{ex} = 514 nm emits at two wavelengths, 570 and 630 nm. The protonated fluorophore emits at 570 nm, and the neutral fluorophore emits at 630 nm. Again, the ratio of the two emissions corresponds to a pH value that is theoretically independent of the concentration of the dye in that compartment. SNARF can be calibrated reliably over the pH range 6.2–9.0. LysoSensor blue DND-167 was used to semiquantitatively investigate the pH in lysosomes. The fluorescence of LysoSensor Blue is dependent on pH. LysoSensor Blue has a functional group that, when deprotonated, leads to a loss of fluorescence of the molecule. The pK of this group is 5.1. Therefore, at pH <5.1, a greater percentage of the dye will be protonated and fluorescent. There is little fluorescence above pH 5.8.

At the end of each experiment, the fluorescence emission of each dye was calibrated with solutions of known pH. For pH calibration of endosomes, the cells were incubated in solutions of 150 mM NaCl, 20 mM Hepes or Mes (depending on the pH of the calibration solution), 5 mM KCl, 1 mM $MgSO_4$ buffered at pH 5, 6, 6.5, and 7, containing monensin (20 μM) and nigericin (10 μM) for 5 min before recording the fluorescence (33). For the pH calibrations of cytosol and nucleoplasm, the cells were incubated in solutions of 140 mM KCl, 10 mM Mops, 5 mM $MgSO_4$, 1 mM $CaCl_2$ buffered at pH 6, 7, and 7.5 containing nigericin (20 μM).

Recycling Compartment pH Measurement

FITC bound to transferrin was used to selectively probe the pH of the endocytic compartment (31, 32). The cells were loaded with 150 μg/ml FITC-transferrin for 30 min. Based on competition binding studies with unlabeled transferrin, this amount of FITC-transferrin specifically labels the recycling endocytic compartment in MCF-7 and MCF-7/ADR cells. The cells were then subsequently washed six times with HBSS with 20 mM Hepes, pH 7.3, and visualized with epifluorescence microscopy (λ_{ex} = 490 and 450 nm, and λ_{em} = 515 nm). The pH was calibrated from the FITC fluorescence as described above.

Lysosome pH

To measure the pH within the lysosomes, the cells were incubated with 5 mg/ml of FITC-dextran 10 kD for 30 min (28), then washed four times in DME with 20 mM Hepes, pH 7.3, and incubated in this medium for 90 min. They were then visualized with epifluorescence with FITC excitation filters (see above). The pH was calibrated from the FITC fluorescence as described above. Alternatively, the cells were incubated with LysoSensor Blue as described above.

pH of the Cytoplasm and Nucleoplasm

The pH within the cytoplasm and nucleoplasm was selectively probed by loading these compartments with SNARF conjugated to dextrans using a procedure referred to as "scrape loading" (34). Briefly, the cells were plated on polystyrene plates at 50% confluence 24–36 h before loading with dextrans. The medium was aspirated, and the cells were rapidly (<10 s) scraped off in the presence of 10 mg/ml of 70- or 10-kD SNARF-dextran and washed in ice-cold media to minimize endocytosis before plating on coverslips as described previously (34). Confocal fluorescence microscopy was used to prepare optical sections through the cell. The fluorescence intensity of the nucleoplasm and cytoplasm could then be quantified. The fluorescence from the SNARF-conjugated dextrans was recorded 24–36 h after scrape loading. The pH was calibrated from the fluorescence as described above.

Immunofluorescence

LAMP-1. For immunolocalization of lysosomes, anti–LAMP-1 serum was used as described previously (35). Cells were fixed with 2% paraformaldehyde in 50 mM phosphate buffer, pH 7.8, containing lysine (9 mg/ml) for 2 h. They were then permeabilized with 0.01% saponin for 5 min. Anti–LAMP-1 sera was used undiluted for 30 min at room temperature. Cells were washed extensively with PBS and then incubated for 15 min with goat anti–mouse secondary antibody Fab fragments conjugated to phycoerythrin at 1:150 dilution at room temperature. Cells were washed in PBS and visualized with the confocal microscope using λ_{ex} = 488 nm.

Results

Adriamycin Distribution in Drug-resistant MCF-7/ADR and Drug-sensitive MCF-7 Cells

The PSS hypothesis predicts that weak base chemotherapeutic drugs should accumulate in the acidic secretory organelles of drug-resistant cells. Adriamycin was chosen as the model chemotherapeutic drug to characterize the subcellular distribution of these agents in drug-sensitive and drug-resistant tumor cells because its natural fluorescence allows it to be tracked visually, and because it is widely ad-
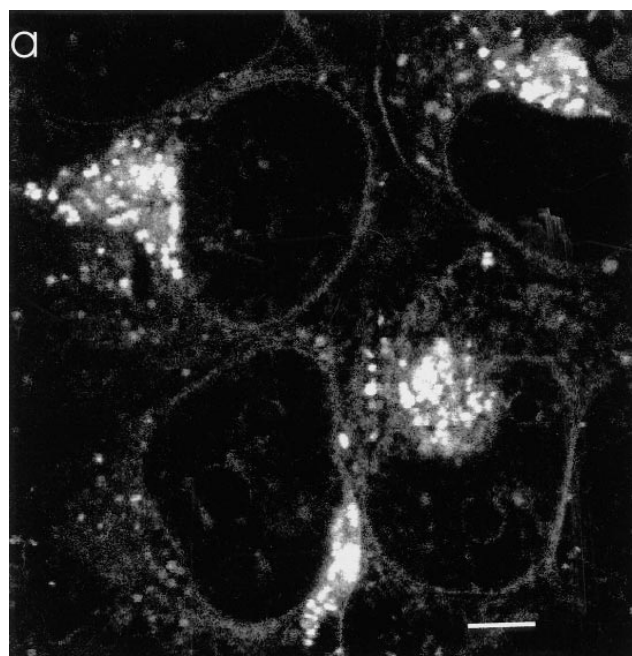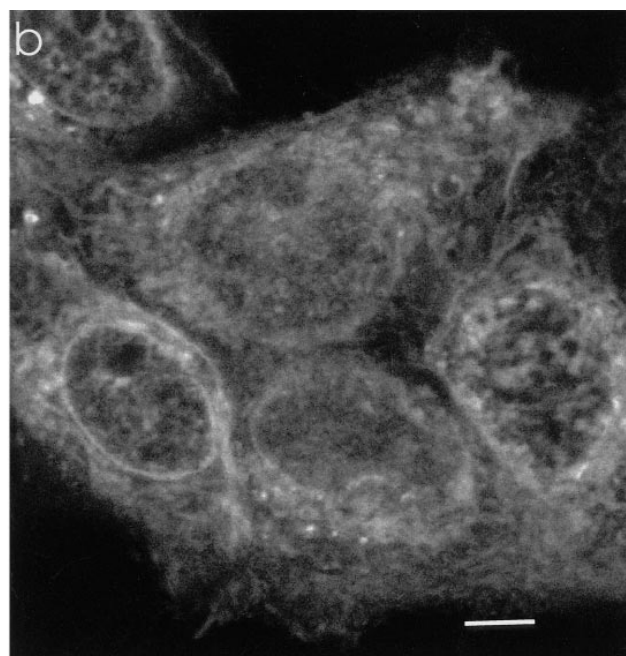
MCF-7/adr (drug-resistant)   MCF-7 (drug-sensitive)

Figure 1. Adriamycin distribution between drug-resistant and drug-sensitive MCF-7 cells. (*a*) In MCF-7/ADR cells, Adriamycin is excluded from the nucleus. It is concentrated in punctate organelles throughout the cytoplasm and a brightly fluorescent region immediately adjacent to the nucleus. This perinuclear labeling is typical for the recycling endosomes and TGN. (*b*) In MCF-7 cells, the fluorescence of Adriamycin is localized diffusely throughout the cytoplasm and nucleoplasm, with little accumulation in any cytoplasmic compartment. Adriamycin is also seen labeling the nuclear envelope. Currently, we do not know if Adriamycin fluorescence is due to accumulation in the nuclear envelope or binding to the adjacent euchromatin. Cells were incubated in the presence of 10 μM Adriamycin as described in Materials and Methods. Scale bar, 5 μm.

ministered in the treatment of many different types of cancers. MCF-7 and MCF-7/ADR cells were used as a pair of drug-sensitive and drug-resistant cell lines, respectively. They are human breast carcinoma cells that are used as an in vitro model system for breast cancer. The drug-resistant MCF-7/ADR cell line is derived from the MCF-7 cell line by selection in the chemotherapeutic Adriamycin (36). MCF-7/ADR cells are also cross-resistant to a number of other chemotherapeutic drugs, including vincristine, vinblastine, and colchicine (36).

In the drug-sensitive MCF-7 cells, Adriamycin fluorescence was seen throughout the cytoplasm and nucleoplasm (Fig. 1 *b*), with some localized increased fluorescence in both the compartments. The slightly reticular distribution of Adriamycin is likely the consequence of its binding to cytoskeleton (37). One of the primary targets for Adriamycin is in the nucleus, where it binds to DNA and inhibits the DNA metabolic enzyme topoisomerase II, thereby blocking DNA replication and transcription (38, 39). In contrast, in the drug-resistant MCF-7/ADR cells, there was little Adriamycin fluorescence in the nucleoplasm and an apparent reduction of fluorescence in the cytoplasm (Fig. 1 *a*). Instead, the drug was found to be accumulated in a perinuclear region and within punctate compartments throughout the cytoplasm.

Adriamycin Colocalizes with the Acidic Compartments of Lysosomes, Recycling Endosomes, and the TGN, in MCF-7/ADR Cells

Since Adriamycin is a weak base, it is predicted to accumulate inside acidic compartments. To determine if it accumulated in the lysosomes, the most acidified cellular compartment, cells were sequentially labeled with LysoSensor Blue DND-167 and Adriamycin. LysoSensor Blue is a membrane-permeable pH probe whose fluorescence emission is reduced significantly at pH >5.8 (see Materials and Methods). Thus, it selectively fluoresces only in the most highly acidic compartments of living cells such as lysosomes. Discrete punctate fluorescence in the cytoplasm was observed in cells incubated with LysoSensor Blue (Fig. 2 *b*). These lysosomes appeared to be distributed somewhat evenly through the cytoplasm. The same cells were then incubated with Adriamycin and excited at 488 nm, and the emission was collected >550 nm (Fig. 2 *c*). LysoSensor Blue is not excited at 488 nm; therefore, it did not interfere with the Adriamycin signal (data not shown). Most lysosomes (Fig. 2 *b, arrows*) were labeled with Adriamycin (Fig. 2 *c, arrows*). In addition to the lysosomal compartment, there was an additional cytoplasmic region adjacent to the nucleus that was heavily labeled with Adriamycin (Fig. 2 *c*).
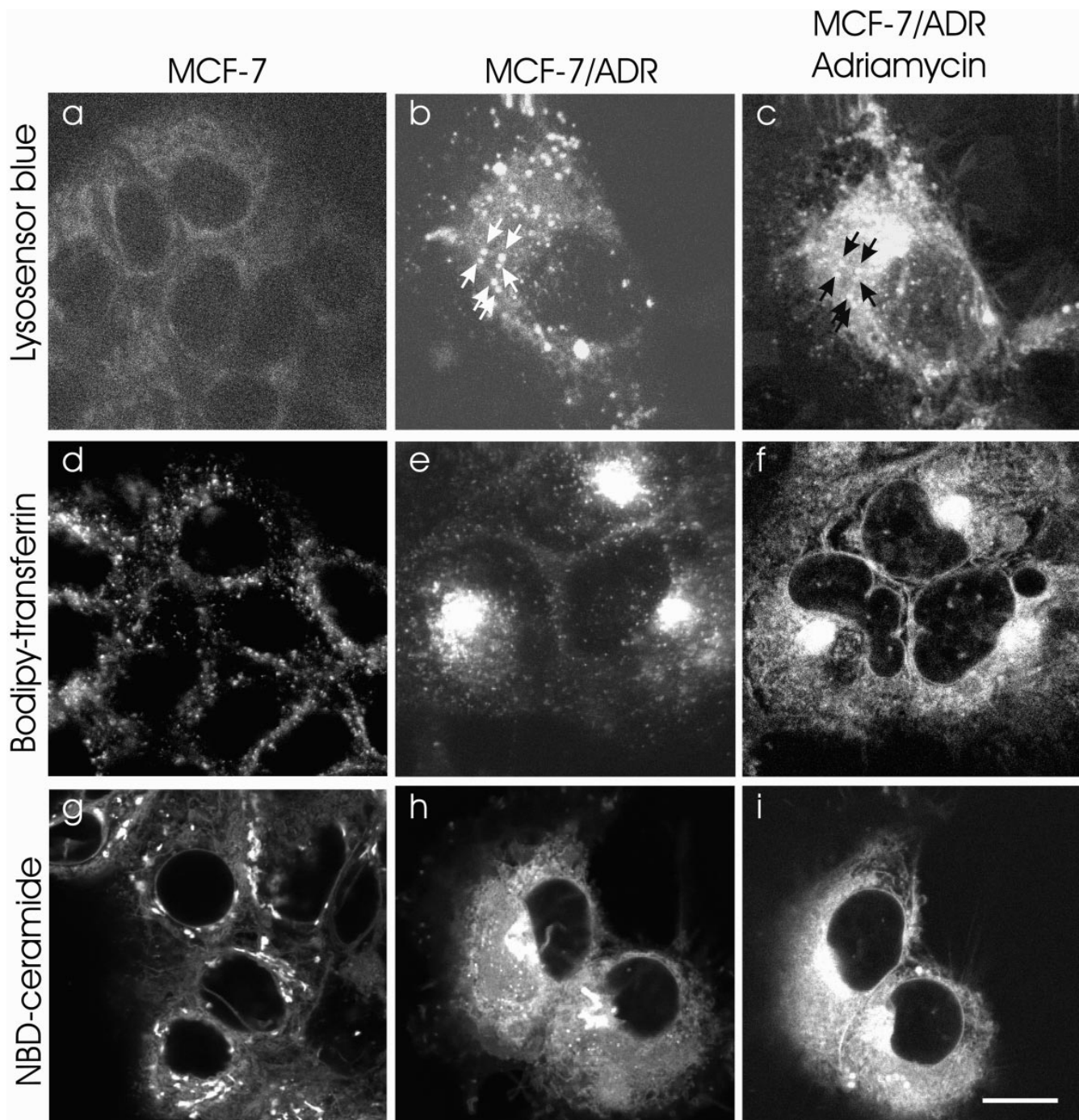
Figure 2. Double labeling of Adriamycin and the perinuclear recycling compartment, TGN, and highly acidified organelles. To characterize the regions that accumulated the Adriamycin in MCF-7/ADR cells, BODIPY-transferrin was used to label the recycling endosomal compartment, NBD-ceramide was used to label the TGN, and LysoSensor Blue was used to label the lysosomes. (*a*) MCF-7 cells accumulate very low levels of LysoSensor Blue, indicating the lack of highly acidified organelles. (*b*) In MCF-7/ADR cells, LysoSensor Blue labels many large punctate peripheral organelles, consistent with lysosomes. *Arrows*, Organelles that colabel with Adriamycin in *c*. (*c*) The same cell was subsequently labeled with 10 μM Adriamycin. Note that the perinuclear compartment, though highly labeled with Adriamycin, has few lysosomes. (*d*) BODIPY-transferrin labels the recycling endosome compartment, which is diffuse and punctate in the cytoplasm of MCF-7 cells. (*e*) BODIPY-transferrin labels the recycling endosome compartment, which is compact and polarized to one side of the nucleus in MCF-7/ADR cells. (*f*) Subsequent labeling of the same cells with Adriamycin also localizes in a perinuclear compartment, which overlaps the compartment labeled in *e*. (*g*) NBD-ceramide labeling of the TGN in MCF-7 cells. The TGN are distributed nonuniformly throughout the cytoplasm. In some cells, the TGN is perinuclear but not polarized to one side of the nucleus. (*h*) NBD-ceramide labeling of the TGN in MCF-7/ADR cells. This compartment is compact and polarized to one side of the nucleus. (*i*) Subsequent labeling of the same cells with Adriamycin also localizes in a perinuclear compartment which overlaps with the TGN compartment labeled in *h*. Cells were either optically sectioned in 0.2-μm slices and optical sections at equivalent distances through the cell were compared, or the images were taken at a single focus which remained unchanged throughout the course of the experiments. The recycling compartment, lysosomes, and TGN were labeled as described in Materials and Methods. Scale bar, 10 μm.

In many cell types, the TGN and the recycling endosome compartment are found adjacent to the nucleus. These two compartments are also known to be acidic (40–42). Therefore, specific fluorescent probes were used to determine if the perinuclear Adriamycin accumulation in the MCF-7/ADR cells colocalized with these compartments. Due to the broad excitation and emission spectrum of Adriamycin, it was not possible to simultaneously label a cell with Adriamycin and available fluorescent markers for endosomes and the TGN. Therefore, colocalization was done by sequential labeling with Adriamycin and the organelle markers.

To examine whether Adriamycin colocalized with the recycling endosome compartment, cells were first labeled with BODIPY-transferrin by receptor-mediated endocytosis. In MCF-7/ADR cells, transferrin labeling revealed that the recycling endosomal compartment has a perinuclear localization (Fig. 2 *e*). The transferrin label was subsequently chased out (half time = 5 min) with unlabeled transferrin. Next, the cells were incubated with Adriamycin for 20 min. In each cell, the region that labeled with BODIPY-transferrin was also labeled with Adriamycin (Fig. 2 *f*). Thus, the Adriamycin accumulation colocalized with the recycling endosomes.

In some cell types, the TGN is in close proximity with the recycling endosome compartment (43, 44). To test if Adriamycin colocalized with the TGN in the MCF-7/ADR cells, the cells were sequentially labeled with Adriamycin and NBD-ceramide, a vital stain for the TGN (45).

A field of cells was labeled with Adriamycin (10 μM) (Fig. 2 *i*). The cells were then washed with Adriamycin-free media until they no longer showed any Adriamycin labeling. Next, the cells were labeled with NBD-ceramide (Fig. 2 *h*). Again, the region labeled with NBD-ceramide was also labeled with Adriamycin. Thus, Adriamycin accumulation is colocalized with the acidic organelles of the drug-resistant MCF-7/ADR cells—the recycling endosome compartment, the TGN, and the lysosomes.

Location of the Lysosomes, Recycling Endosome Compartment, and the TGN in Drug-sensitive MCF-7 Cells

There was little organellar labeling of Adriamycin in drug-sensitive MCF-7 cells (Fig. 1 *b*). Therefore, the presence and distribution of each of these organelles in these cells were tested to determine if the organelles were either missing or present but failing to accumulate chemotherapeutic drugs. The distribution of the recycling endosome compartment was probed with BODIPY-transferrin, and the TGN was probed with NBD-ceramide (45). In the drug-sensitive MCF-7 cells, both the recycling endosome compartment (Fig. 2 *d*) and the TGN (Fig. 2 *g*) were distributed throughout the cytoplasm. Their distribution was very different from the MCF-7/ADR cells, where both compartments were distinctly perinuclear in location and polarized to one side of the nucleus. Furthermore, unlike the MCF-7/ADR cells, in the MCF-7 cells, Adriamycin was not concentrated in any of these compartments (Fig. 1 *b*).
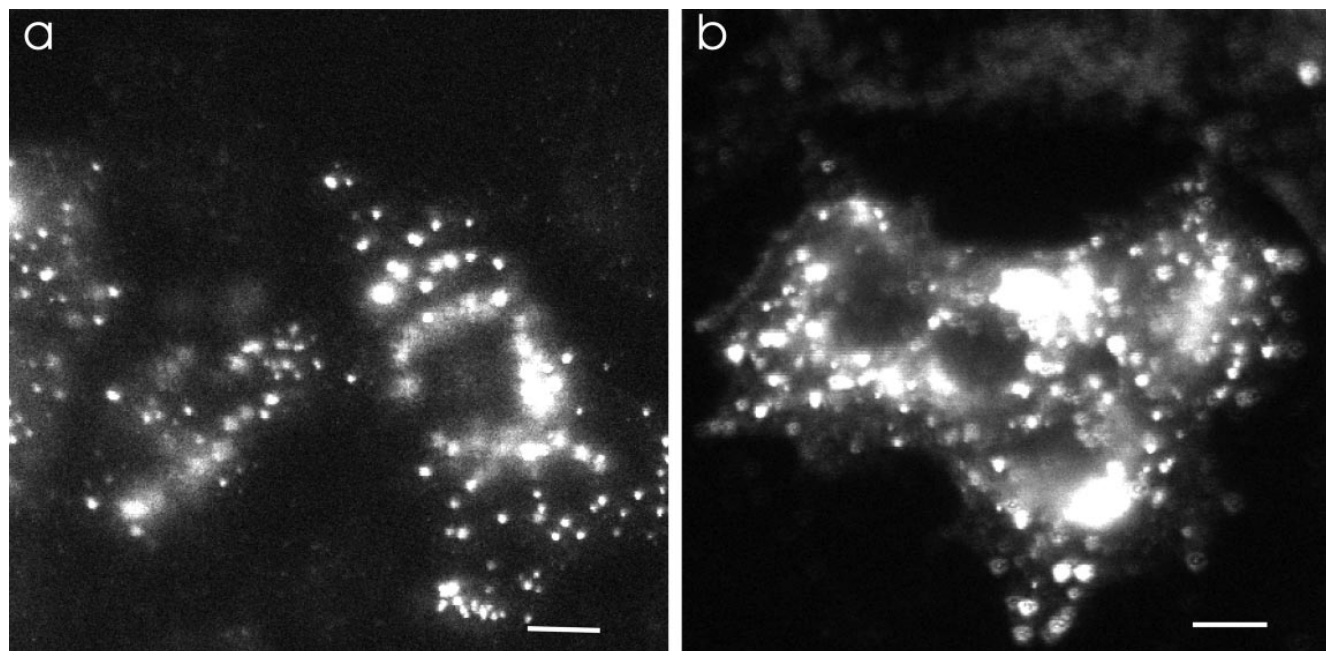
Figure 3. Distribution of lysosomes in MCF-7 and MCF-7ADR cells. LAMP-1 is a membrane protein of lysosomes which is found in punctate organelles throughout the cytoplasm of (*a*) MCF-7/ADR cells and (*b*) MCF-7 cells. Analysis of large fields of MCF-7 and MCF-7/ADR cells did not reveal any significant differences in the phenotypic distribution or number of lysosomes per cell. MCF-7/ADR and MCF-7 cells were fixed in paraformaldehyde as described in Materials and Methods. Scale bar, 10 μm.

ADRIAMYCIN (pK8.3)

DAUNOMYCIN (pK8.4)

VINBLASTINE (pK7.4)
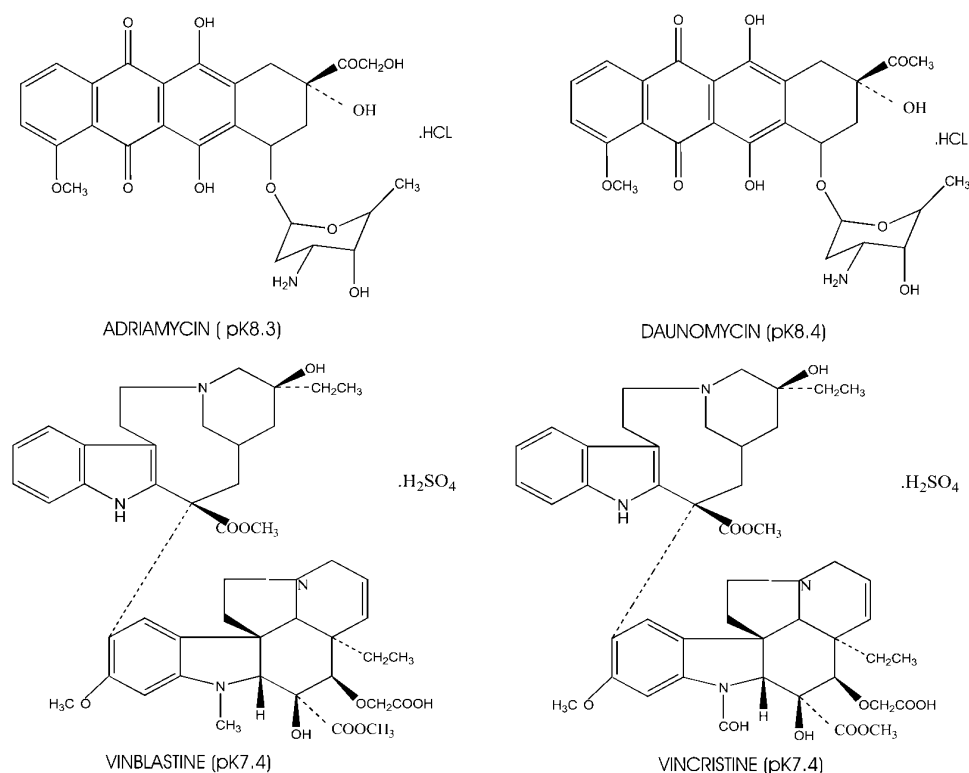
VINCRISTINE (pK7.4)

Figure 4. The chemical structures of four widely used chemotherapeutic drugs. Adriamycin and Daunomycin belong to the anthracycline class of compounds; vincristine and vinblastine are representative of the vinca alkaloids. Note that these drugs all are weak bases, with pK_a between 7.2 and 8.4, and are all partially hydrophobic and partially hydrophilic. This property allows them to diffuse across lipid bilayers.

The distribution of lysosomes in MCF-7 and MCF-7/ADR cells was compared using immunofluorescence for the lysosomal integral membrane protein LAMP-1 (46). LAMP-1 was chosen as an indicator rather than LysoSensor Blue because LysoSensor Blue requires acidified lysosomes for labeling. Both MCF-7/ADR cells (Fig. 3 *a*) and MCF-7 cells (Fig. 3 *b*) had punctate LAMP-1–labeled compartments in the cytoplasm. There was little qualitative or quantitative difference in the distribution of LAMP-1 labeling between the two cell types. In some MCF-7 and MCF-7/ADR cells, there was also a perinuclear staining for LAMP-1 which could be indicative of lysosomes or TGN since this membrane protein is sorted to the lysosomes from the TGN. Together, the results demonstrate that the recycling endosomes, TGN, and lysosomes are present in the MCF-7 cells but do not accumulate Adriamycin.

Subcellular pH Profiles of MCF-7 and MCF-7/ADR Cells

Many of the chemotherapeutic drugs, such as Adriamycin, vincristine, vinblastine, daunomycin, and mitoxantrone, are heterocyclic amines (see Fig. 4) (15, 16, 47). With pK_a values at or just above physiological pH, they are weak bases and are membrane permeable only in the noncharged form. This has been tested empirically in single-membrane model systems of liposomes (48) and anucleate red blood cells (18, 19). In liposomes in which the lumenal compartments are more acidic relative to the external medium, there is a net lumenal accumulation of Adriamycin. The

magnitude of this pH-dependent lumenal accumulation closely approximates theoretical calculations. For example, Adriamycin with pK_a of 8.3 accumulates ~100-fold in a liposome with a lumenal pH of 6 and an external pH of 8 (48). As shown above (Fig. 2, *b*, *c*, *e*, *f*, *h*, and *i*), Adriamycin accumulation colocalized with each of the acidic organelles of the cell. However, Adriamycin did not accumulate within these same organelles in the drug-sensitive MCF-7 cells. Therefore, the pH was examined in the cytosol and organelles of MCF-7 and MCF-7/ADR cells to determine whether the failure to concentrate Adriamycin in the organelles of MCF-7 cells was the consequence of a failure to acidify.

Qualitative pH Profile Monitored with Acridine Orange. Acridine orange is a fluorescent weak base that is used frequently as a probe for acidification of organelles (49, 50). When accumulated in high concentrations in acidic compartments, its emission shifts from green to red (50). MCF-7 and MCF-7/ADR cells were incubated with acridine orange. In drug-resistant MCF-7/ADR cells, there was a red-orange fluorescence in discrete cytoplasmic organelles (Fig. 5 *a*), indicating acridine orange accumulation and thus an acidified compartment. This fluorescent pattern is similar to that observed in various nontransformed cells, such as the MCF-10F cells (Fig. 5 *c*), parietal cells (51), paramecium (52), pituitary cells (53), and *Xenopus* oocytes (54). The MCF-10F cells originated from a female patient with normal nonmalignant breast tissue. These cells have a normal or near-normal karyotype (55). The cytosol and nucleoplasm of MCF-10F cells show a diffuse green fluorescence

with discrete punctate red-orange organelles distributed throughout the cytoplasm.

In contrast, acridine orange in the MCF-7 cells had significantly fewer red-orange fluorescent compartments, indicating many fewer acidic vesicles (Fig. 5 *b*). The fluorescence of acridine orange does not give any information as to the identity of the acidic compartments or the absolute value of the pH within these compartments. Therefore, subsequent experiments used ratiometric pH probes targeted to specific organelles and whose pH could be calibrated in situ. A similar qualitative difference in the distribution of acridine orange has also been observed in K-562 drug-sensitive and drug-resistant human erythroblastoma cells (26).

pH within the Recycling Endosome Compartment. To measure the pH within the recycling endosome compartment, the cells were loaded with FITC-transferrin. FITC is a fluorophore sensitive to pH within the range 5.0–7.0 (56). It was found that the drug-resistant MCF-7/ADR cells had an average recycling endosome compartment pH of 6.1 ± 0.1, whereas the drug-sensitive MCF-7 cells had an average recycling endosome compartment pH of 6.6 ± 0.1 (Table 1). A similar quantitative difference in endosome pH was seen in the drug-resistant and drug-sensitive MDA-231 human breast tumor cell lines (unpublished observations).

pH within the Lysosomes. The pH of the lysosomes in MCF-7 and MCF-7/ADR cells was measured with LysoSensor Blue. The fluorescence of this probe is strongest at pH <5.1 and disappears at pH >5.8. In most MCF-7 cells, there were few acidic compartments (10.6 ± 5.5 per cell, $n = 78$), and in some cells, there was virtually no fluorescence above background (Fig. 2 *a*), suggesting there are few compartments with pH values <5.8. In contrast, there were significantly more punctate fluorescent organelles (43.0 ± 10, $n = 15$) when the MCF-7/ADR cells were labeled (Fig. 2 *b*). The pH of the lysosomes in MCF-7/ADR cells was measured independently with FITC conjugated to dextran, a fluid phase probe that accumulates in lysosomes (28). The average pH obtained for the lysosomes using this method was pH 5.1 ± 0.1 (Table 1). This method could not be used to measure the pH of lysosomes in MCF-7 cells because of slow delivery of the fluid phase marker to the lysosome (unpublished observations). However, the lack of acidic lysosomes as monitored by LysoSensor Blue in MCF-7 cells correlated with the lack of punctate Adriamycin fluorescence (Fig. 1 *b*) as well as with the lack of punctate red fluorescence from acridine orange (Fig. 5 *b*) within the cytoplasm of these cells. While LysoSensor Blue failed to label lysosomes of MCF-7 cells (Fig. 2 *a*), immunolocalization indicates that these cells have numbers of lysosomes comparable to MCF-7/ADR cells (Fig. 3). This indicates that the lysosomes are present in these drug-sensitive cells but fail to acidify.

pH within the Cytoplasm and Nucleoplasm. Previous work showed that many drug-resistant cell lines have higher total cellular pH than their drug-sensitive counterparts (2, 22–25, 57). In addition, changing the cellular pH by shifting the pCO$_2$ of the media results in a corresponding shift in cytoplasmic Adriamycin concentration (25). When Adriamycin is incubated with cells, the first intracellular compartment into which it diffuses is the cytosol. The cytosolic pH determines the proportion of Adriamycin that will be protonated and unable to diffuse back across the plasma membrane.

These previous cellular pH measurements were made with cell-permeant pH probes (e.g., 2′7′-bis(2-carboxyethyl)-5(6) carboxy fluorescein acetoxymethylester, and SNARF-acetoxymethylester) that are deesterified in the cytosol. However, there are several reasons why these are not good probes for cytosolic pH. First, some of the probes are internalized by endocytosis. Thus, they would be reporting a weighted sum of cytosolic and endosomal pH. Second, they accumulate in intracellular organelles which contain esterases and organic anion transporters that have been proposed to transport these probes (58). Therefore, their fluorescence is a weighted average of the cytosolic and organellar pH. Third, these probes have been suggested as substrates for Pgp (59). This would complicate considerably comparisons of results between the MCF-7 and MCF-7/ADR cells (which express Pgp).

To specifically measure the cytosolic and nucleoplasmic pH, an ideal probe would be large, membrane impermeable, and rapidly and selectively introduced into the cytosol. SNARF, conjugated to a dextran of 10 or 70 kD, was loaded into the cytosol by scraping adherent cells rapidly off the surface of polystyrene (34). The scraping causes a

Table 1. *Summary of Endosome, Lysosome, Cytosol, and Nucleoplasm pH*

| Compartment | Endosome | Lysosome | Lysosome | Cytosol | Nucleoplasm |
Probe	FITC-transferrin	FITC-dextran	LysoSensor Blue	SNARF–70-kD dextran	SNARF–10-kD dextran
pH MCF-7	6.6 ± 0.1	ND	>5.8	6.75 ± 0.3	7.1 ± 0.1
ΔpH to cytosol	0.15	ND	<0.9	–	−0.35
ΔpH to media	0.7	ND	<1.5	0.55	0.2
pH MCF-7/ADR	6.1 ± 0.1	5.1 ± 0.1	<5.8	7.15 ± 0.1	7.2 ± 0.1
ΔpH to cytosol	1.05	2.05	>1.35	–	−0.05
ΔpH to media	1.2	2.2	>1.5	0.15	0.1
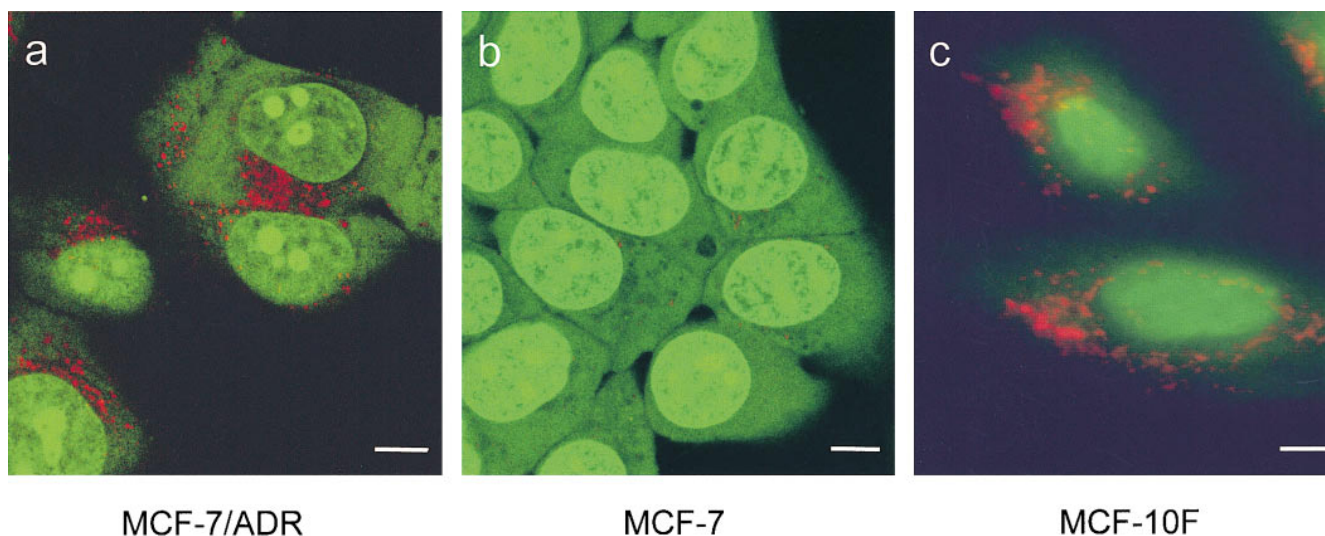
Figure 5. There is a lack of acidification within the subcellular compartments of drug-sensitive MCF-7 cells as assayed by acridine orange. Acridine orange is a weak base that fluoresces red when it accumulates in acidic compartments. (*a*) In MCF -7/ADR cells, there are many punctate red-orange fluorescing compartments throughout the cytoplasm, which is indicative of acidic organelles. (*b*) In MCF -7 cells, there is little red-orange fluorescence from acridine orange. This is diagnostic for few acidified organelles. Note also that the nucleus of MCF-7 cells takes up a greater amount of acridine orange than the nucleus of MCF-7/ADR cells. (*c*) In MCF-10F cells, a nontransformed human breast epithelial cell line, there are also many punctate red-orange fluorescing compartments distributed throughout the cytoplasm, indicative of acidic organelles. *a* and *b* were observed using confocal microscopy; *c* was observed under epifluorescence. Scale bar, 5 μm.

temporary shearing of the plasma membrane, which allows the impermeant macromolecules to diffuse into the cytosol. Since the pH probe SNARF is conjugated to a dextran, once introduced into the cytosol it does not cross cellular membranes. To measure the pH within the cytosol, the probe was conjugated to a 70-kD dextran which is too large to pass through the nuclear pores (Fig. 6 *a*). To mea-

sure the pH within the nucleoplasm, the probe was conjugated to a 10-kD dextran, which is too large to cross membranes into organelles but still small enough to pass through the nuclear pores (Fig. 6 *b*).

These measurements show that MCF-7 cells have an average cytosolic pH of 6.75 ± 0.3, which is 0.4 U lower than the cytosolic pH of MCF-7/ADR cells (pH 7.15 ±
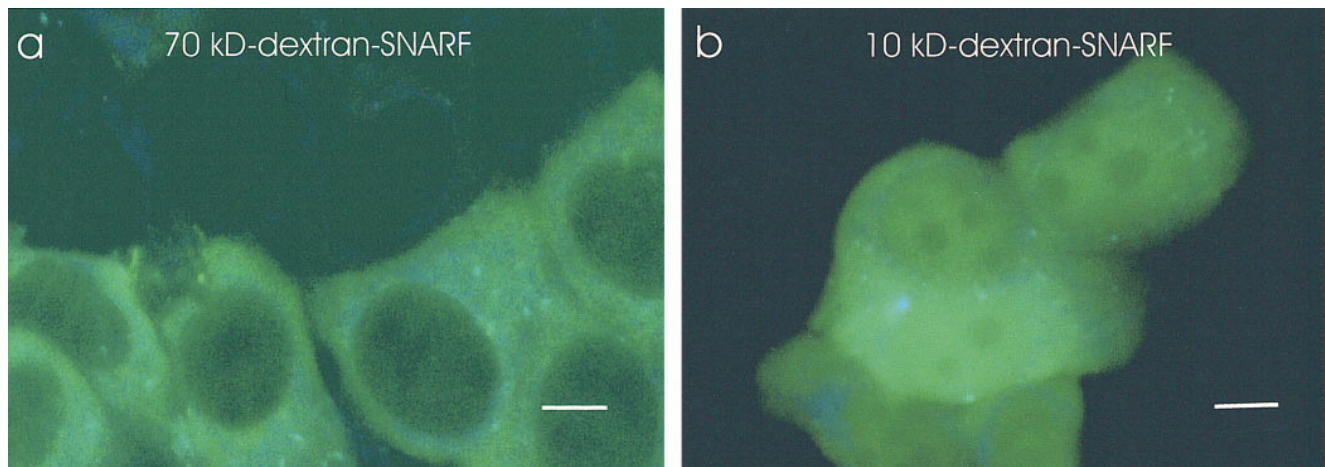
Figure 6. Specific loading of a pH probe into the cytosol of MCF-7 cells. Cells were scrape loaded with SNARF-dextran as described in Materials and Methods. Scale bar, 5 μm. (*a*) 70-kD SNARF-dextran loaded into MCF-7 cells. The fluorescence was excluded from the nucleoplasm and was observed as diffuse cytoplasmic fluorescence. Conjugated to a dextran, it cannot cross internal membranes. Thus, it specifically reports the pH of the cytosol. (*b*) MCF-7 cells were loaded with a 10-kD SNARF-dextran. The probe is present in both the cytosol and nucleoplasm. The distribution of these probes in MCF-7/ADR cells is similar. Note that in some cells, the SNARF-dextran has a punctate distribution in some areas of the cytoplasm, which may be due to an aberrant aggregation of SNARF-dextran. All pH measurements were taken from a region of cytoplasm where there was no aggregation of the probe.
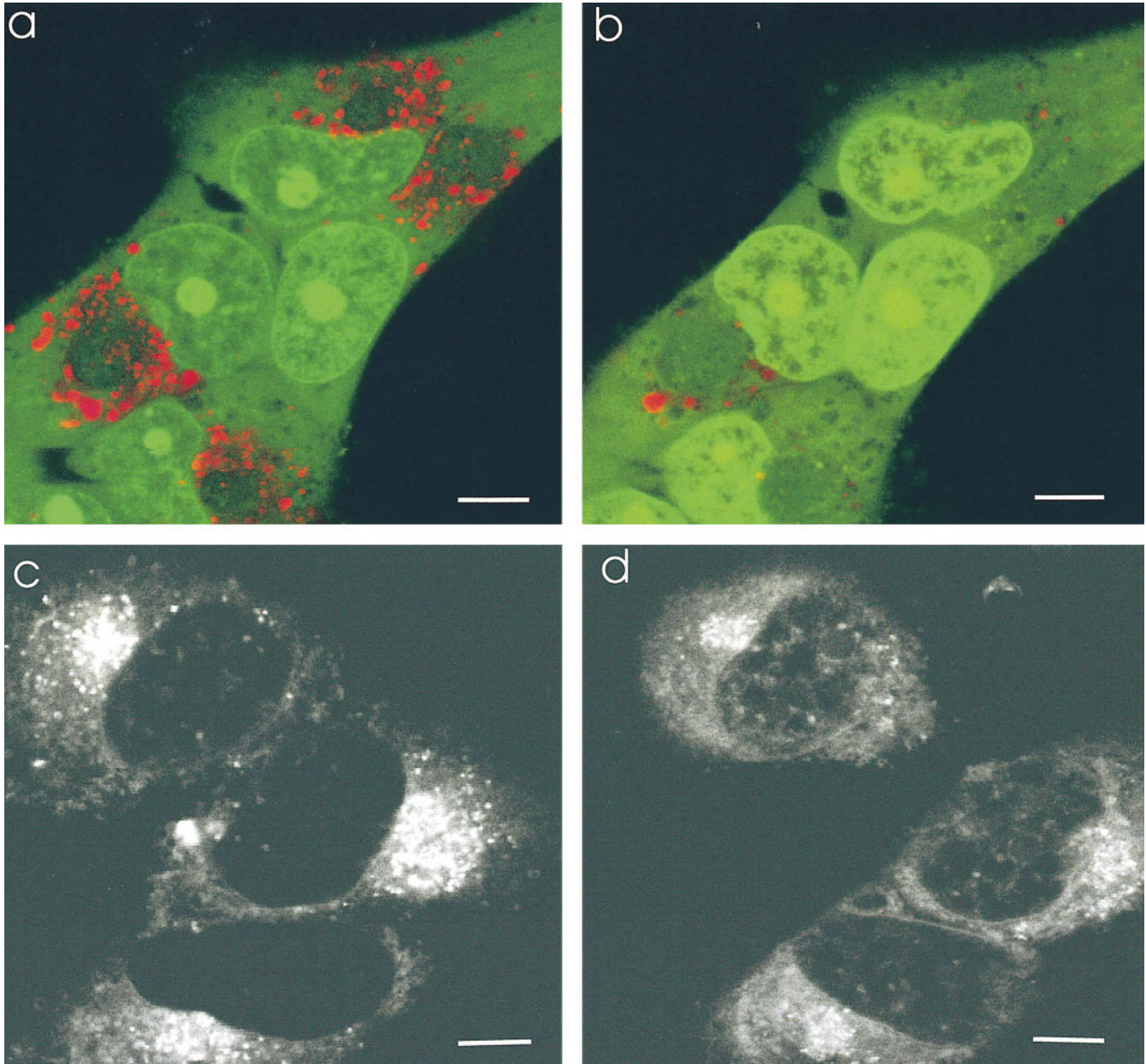
Figure 7. Effect of monensin on acidification and Adriamycin distribution in MCF-7/ADR cells. Monensin disrupts the acidification of subcellular compartments in drug-resistant MCF-7/ADR cells and redistributes Adriamycin to the nucleus. Scale bar, 5 μm. (*a*) MCF-7/ADR cells were incubated with acridine orange (6 μM) as described in the citation to Fig. 4. There is punctate red-orange fluorescence throughout the cytoplasm, indicative of acidified organelles. (*b*) Monensin (5 μM) was added to the solution bathing the cells in *a*. 30 min after addition of monensin, there was a loss of the red-orange fluorescence observed within cytoplasmic compartments. This is indicative of a loss of acidification. (*c*) Adriamycin was incubated with MCF-7/ADR cells as described in the citation to Fig. 1. Adriamycin is again observed to accumulate in a perinuclear compartment that colocalizes with the lysosomes, recycling endosomes, and TGN compartments (see Fig. 2). (*d*) Monensin was added to the media bathing the cells in *c*. After 30 min, the perinuclear accumulation of Adriamycin has decreased, and instead Adriamycin is found to accumulate within the nucleus. The distribution of Adriamycin now resembles that seen in drug-sensitive MCF-7 cells (Fig. 1 *b*).

0.1) when the extracellular medium is buffered at pH 7.3 (Table 1). The pH of the nucleoplasm in both cell types was 0.1–0.3 pH U more alkaline than the cytosol pH (Table 1). This is consistent with another recent report, which finds a more alkaline nucleoplasmic pH (60). The higher cytosolic pH of MCF-7/ADR cells results in a lower plasma membrane ΔpH and contributes to a greater organellar ΔpH. This is consistent with the hypothesis that the distribution of the weak base Adriamycin (Fig. 1) is affected by pH gradients across membranes.

Effect of Ionophores and Blockers of the H$^+$-ATPase on the Response of MCF-7/ADR Cells to Adriamycin. These results demonstrate a large difference in the subcellular pH profile between the drug-resistant and drug-sensitive cell types
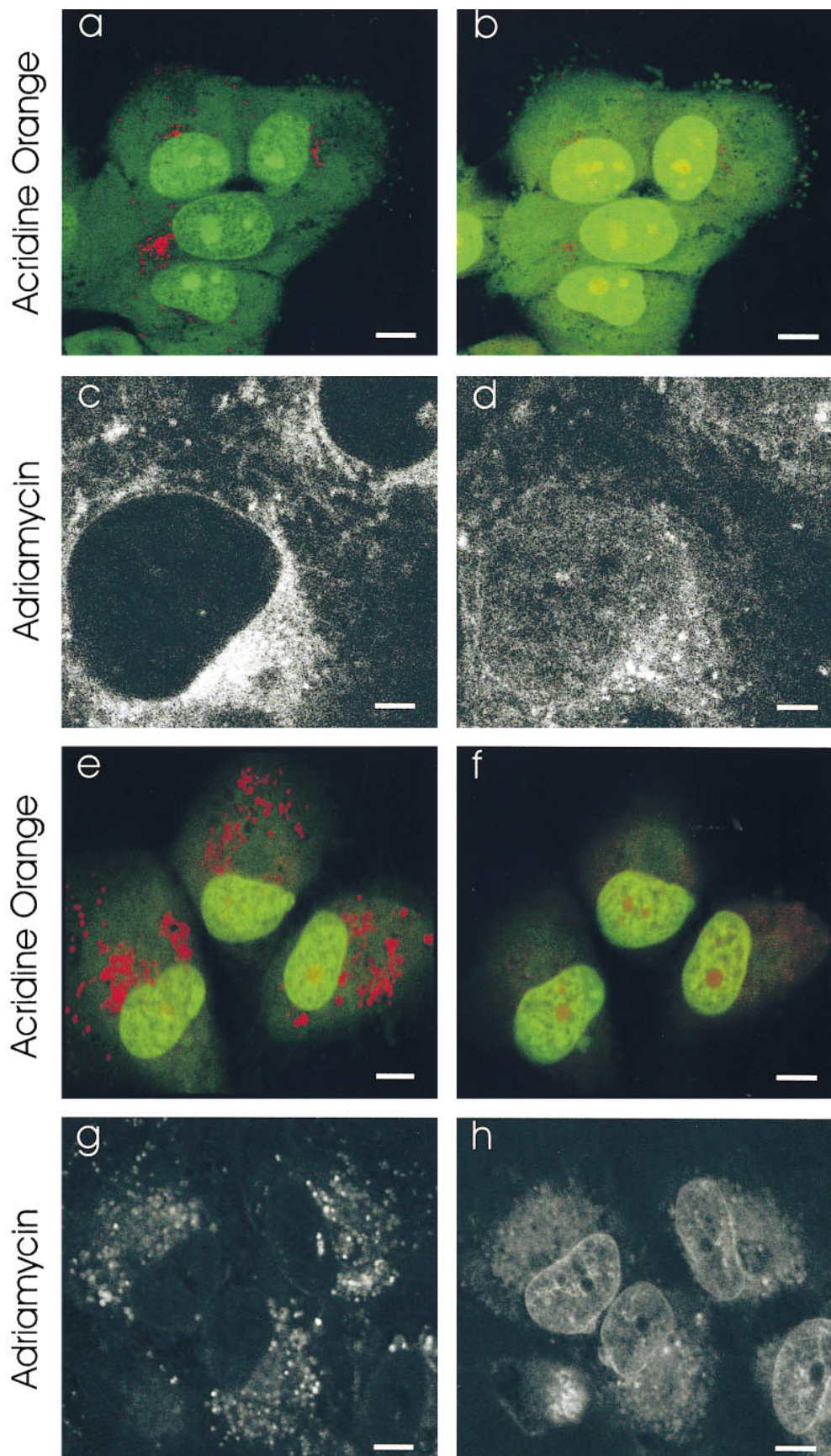
Figure 8. Effect of inhibitors of the vacuolar H^+-ATPase on acidification and Adriamycin distribution in MCF-7/ADR cells. Inhibitors of the vacuolar proton ATPases disrupt the acidification of drug-resistant MCF-7/ADR cells and redistribute the Adriamycin to the nucleus as assayed by laser-scanning confocal microscopy. Scale bar in *c* and *d* is 2 μM, and in *a, b,* and *e–h* is 5 μM. (*a*) MCF-7/ADR cells were labeled with acridine orange as in the citation to Fig. 5. The punctate red-orange fluorescence in the cytoplasm is diagnostic for acidified organelles. (*b*) The same cells as in *a,* 30 min after addition of bafilomycin A1 (500 nM). Note the disappearance of punctate red-orange cytoplasmic fluorescence, indicative of reduced acidification. (*c*) MCF-7/ADR cells were incubated with Adriamycin as in the citation to Fig. 1. The Adriamycin fluorescence is observed within punctate cytoplasmic organelles which colocalize with lysosomes (see Fig. 2, *g–i*) and with a perinuclear compartment which colocalizes with the TGN (see Fig. 2, *d–f*) and the recycling endosomes (see Fig. 2, *a–c*). (*d*) The same cells as in *c,* 30 min after addition of bafilomycin A1 (500 nM). The fluorescence of Adriamycin is decreased substantially in all cytoplasmic compartments and increased in the nucleoplasm. (*e*) Acridine orange–labeled MCF-7/ADR cells as in *a.* (*f*) The same cells as in *e* 30 min after inclusion of concanamycin (100 nM) in the incubation media. The punctate red-orange fluorescence from acridine orange accumulation is almost completely dissipated. (*g*) Fluorescence of Adriamycin in MCF-7/ADR cells. (*h*) The same cells as in *g* 30 min after inclusion of concanamycin (100 nM) in the incubation media. There is a substantial decrease of Adriamycin fluorescence in punctate cytoplasmic organelles and pericentriolar compartment. In contrast, there is significant increase of Adriamycin fluorescence in the nucleus.

(Table 1). The PSS hypothesis predicts that these differences in acidification are causally related to the drug-resistance phenotype. As a test of this hypothesis, the subcellular pH profile of drug-resistant MCF-7/ADR cells was changed to resemble that of drug-sensitive MCF-7 cells while monitoring the distribution of the chemotherapeutic drug Adriamycin. To do this, the sodium/proton exchanger monensin, which dissipates pH gradients across all membranes (21, 61, 62), and the vacuolar proton ATPase inhibitors bafilomycin A1 and concanamycin A (62, 63) were used to block acidification. Acridine orange–labeled MCF-7/ADR cells (Fig. 7 *a*) when treated with monensin (Fig. 7 *b*) did not exhibit the red spectral shift within the vesicles, indicating the loss of acidification in these compartments. Similar results were seen with the potassium/proton exchanger nigericin (data not shown).

These experiments were repeated with bafilomycin A1 and concanamycin A, which specifically block the proton ATPase. Thus, their mechanism of inhibiting the acidification of endosomes, lysosomes, and TGN is totally different from the ionophores monensin and nigericin. The punctate red acridine orange labeling of acidic organelles in MCF-7/ADR cells (Fig. 8, *a* and *e*) was lost after incubation with bafilomycin A1 (Fig. 8 *b*) or concanamycin A (Fig. 8 *f*). Neither of these agents have any direct effect on the fluorescent properties of acridine orange (data not shown) and, unlike monensin or nigericin, they do not affect membrane permeability.

The distribution of Adriamycin in MCF-7/ADR cells (Fig. 7 *c*, and Fig. 8, *c* and *g*) was monitored upon addition of either monensin (Fig. 7 *d*), bafilomycin A1 (Fig. 8 *d*), or concanamycin A (Fig. 8 *h*). Treatment with any of the three different agents produced a similar redistribution of Adriamycin: a decrease in the punctate cytoplasmic compartments and a diffuse increase across the cytoplasm and nucleoplasm. This distribution of Adriamycin in cells where organelle acidification is blocked is similar to that observed in the drug-sensitive MCF-7 cells (Fig. 1 *b*).

Discussion

Most chemotherapeutic agents have sites of action in the nucleus or in the cytosol. Therefore, their toxicity depends upon their concentration in either of these two compartments. The PSS hypothesis proposes that the concentration of weak base chemotherapeutic drugs in both the cytosol and nucleoplasm is regulated by the ability of cytoplasmic organelles to sequester the drugs away from the cytosol. The PSS hypothesis is based on the assumption that chemotherapeutic drugs entering acidic organelles should become protonated, thereby sequestered from the cytosol, and secreted. We find that Adriamycin colocalizes on the light microscopic level with the acidic organelles of living drug-resistant MCF-7/ADR cells, including the lysosomes, recycling endosome compartment, and the TGN. Our result is consistent with an ultrastructural study of drug-resistant NIH 3T3

cells, which showed that the Golgi compartment and lysosomes were labeled by a photoprecipitate of Adriamycin (14).

The results presented here demonstrate two aberrations of cellular pH regulation in the MCF-7 drug-sensitive tumor cell line. First, there is a failure to acidify organelles as measured both qualitatively (Fig. 5, and reference 21) and quantitatively (Table 1). Second, we have found that the cytosol in MCF-7 cells is 0.4 pH U more acidic than the cytosol of MCF-7/ADR cells. As described below, both of these features will increase the concentration of chemotherapeutic drugs in the cytosol and nucleoplasm of drug-sensitive tumor cells relative to the concentrations in drug-resistant or nontransformed cells. We have observed similar results on organellar acidification in the SW-48 human colon cell line and the MDA-231 (estrogen receptor–negative) human breast cancer line, and qualitatively similar observations have been reported for the K-562 erythroblastoma leukemia cell line (26). Chemotherapy relies upon tumor cells being more sensitive to chemotherapeutic drugs than nontransformed cells. We propose that one factor that might contribute to this enhanced sensitivity in these drug-sensitive cells is a failure of the PSS mechanism.

Effects of Plasma Membrane ΔpH on Drug Distribution. The pH gradient across the plasma membrane of MCF-7 cells is 0.55 U, whereas in drug-resistant MCF-7/ADR cells, it is 0.15 U. Therefore, at equilibrium conditions, there will be ~2.5-fold greater accumulation of Adriamycin in the cytosol of MCF-7 cells than in that of MCF-7/ADR cells.

Effects of Organelle Membrane ΔpH on Drug Distribution. The pH gradients across the organelles of the MCF-7 cells were almost zero (Table 1). Thus, the organelles could not accumulate chemotherapeutic drugs. In contrast, the pH gradient between the recycling endosome compartment and the cytosol of MCF-7/ADR is calculated to be an average of 1.0 pH U, which would cause a 10-fold accumulation in this organelle. The ΔpH between the lysosome and cytosol in MCF-7/ADR cells is <2.0 pH U. Thus, the lysosomes of MCF-7/ADR cells should accumulate at least 100-fold more Adriamycin than the cytosol.

If the distribution of Adriamycin reached an equilibrium, the cytosolic concentration would be solely dependent on the ΔpH across the plasma membrane and extracellular drug concentration. Acidic organelles would accumulate high levels of drugs, but could not lower the cytosolic concentration. However, a large body of work has shown that many acidic organelles, including the TGN and recycling endosomes, continuously secrete their contents by exocytosis. This active process, if fast relative to the diffusion of extracellular drug into the cytosol, will keep cytosolic and nuclear drug levels low. Drug concentrations would not reach equilibrium distribution but would remain at a steady state due to the continuous cycling of acidic organelles. Thus, organellar acidification would lower the concentration of Adriamycin in the cytosol and nucleoplasm of drug-resistant and nontransformed cells. In fact, this mechanism may account for the difference in Adriamycin distribution

we observed between MCF-7 and MCF-7/ADR cells (Fig. 1). In drug-resistant MCF-7/ADR cells, Adriamycin was sequestered within subcellular organelles, decreasing the drug concentration within the nucleoplasm and, accordingly, in the cytosol as well. (The high density of organelles throughout the cytoplasm makes it impossible to resolve Adriamycin fluorescence selectively from the cytosol. As a first approximation, we assume that the nucleoplasmic concentration reflects the free cytosolic concentration, since Adriamycin should be freely permeable through both the nuclear envelope and the nuclear pores, whose size cut-off is 25 nm [64]). In drug-sensitive cells, in the absence of an organellar mechanism for sequestration, a greater percentage of incoming Adriamycin remained in the cytosol with access to binding sites within the nucleus.

The PSS hypothesis proposes that cytosolic/nucleoplasmic drug concentrations are a function of the ΔpH and drug permeability of the plasma membrane, the ΔpH and drug permeability of the organellar membrane, and the rate of exocytosis. Hence, nuclear/cytosolic drug levels would be increased by (*a*) elevated plasma membrane ΔpH, which would increase cytosolic drug accumulation; (*b*) decreased organellar ΔpH, which would decrease sequestration; and (*c*) decreased rate of secretion, which would permit the drug levels to equilibrate across organelle membranes. The PSS hypothesis predicts that at a steady state, dissipation of plasma membrane ΔpH will decrease drug sensitivity, whereas dissipation of organellar ΔpH and/or decreasing the rate of secretion will increase drug sensitivity.

MDR in tumors could stem from a number of cell biological changes. The most frequently proposed mechanism for MDR in tumors is a plasma membrane–based efflux pump that uses ATP to transport chemotherapeutic drugs (4). This idea is based on studies in cell lines that express two of the proteins implicated in multidrug resistance, Pgp and MRP. The evidence includes the observations that (*a*) addition of azide to these cells increases nuclear accumulation of chemotherapeutic drugs; (*b*) both Pgp and MRP have ATP-binding domains; and (*c*) chemotherapeutic drugs modified with photoactive groups can be used to label Pgp. The PSS mechanism tested in this paper may be an additional mechanism for drug resistance working separately from the Pgp and MRP drug-efflux pumps.

It is also possible that both Pgp and MRP contribute to the PSS mechanism by affecting organelle pH. Indeed, it has been demonstrated that transfection of cells with Pgp results in an alkaline shift of the cytosolic pH (23) and total cellular pH (24) consistent with the pH shift seen in resistant cells (Table 1). One clue to the mechanism for this pH shift may come from the structural homology between Pgp, MRP, and the ATP–binding cassette family of proteins, which includes the cystic fibrosis transmembrane conductance regulator, a chloride channel expressed in lung epithelial cells. In cells defective in cystic fibrosis transmembrane conductance regulator, there is reduced acidification of the TGN and recycling endosome compartments (65). Acidification of organelles requires a proton

ATPase. However, proton pumping alone is not sufficient to acidify to levels seen in organelles such as endosomes and lysosomes. The membrane potential caused by the proton gradient blocks the activity of the proton ATPase. Thus, anion channels are necessary to dissipate the membrane potential and keep the proton ATPase pumping protons (40, 66). Both Pgp and MRP have been observed to be components of intracellular membranes (67, 68). They might either form ion channels or modify the activity of ion channels (69–73). If the MCF-7 cells were missing a counterion transport, this would limit acidification of the organelles. The presence of Pgp or MRP may facilitate a counterion transport, allowing restoration of acidification within these organelles in the MCF-7/ADR cells. However, there is still disagreement over whether Pgp forms an ion channel (69, 74).

There are differences in the pH gradients across both the plasma membrane and organellar membranes between drug-sensitive and drug-resistant cells (Table 1). Results presented here indicate that the cellular organelles are critical determinants of cellular sensitivity to chemotherapeutic drugs that are weak bases. Monensin disrupts pH gradients across all cellular membranes. Dissipation of plasma membrane ΔpH should decrease the cytosolic concentration of adriamycin in MCF-7/ADR cells, and conversely, dissipation of organellar ΔpH should increase cytosolic and nucleoplasmic adriamycin. The observation that monensin increases the nucleoplasmic concentration of Adriamycin (Fig. 7 *d*) and increases substantially the sensitivity of MCF-7/ADR cells to Adriamycin (21) suggests that organellar pH gradients make a greater contribution to Adriamycin distribution than plasma membrane pH gradients. Further, both bafilomycin A1 and concanamycin A, which specifically block the vacuolar proton ATPase in endosomes and lysosomes (62, 63) and TGN of eukaryotic cells (42), increase adriamycin levels in the nucleus (Fig. 8, *d* and *h*). Thus, the drug-resistant phenotype—both sequestration of drugs into cytoplasmic organelles and the sensitivity of cells to the weak base chemotherapeutic drugs—is causally dependent upon organelle acidification. The pH gradient across the plasma membrane may make significant contributions to the sensitivity of drug-resistant cells to non-weak base chemotherapeutic drugs such as colchicine and taxol. The binding of colchicine to tubulin is pH dependent and is favored at more acidic pH (75). Similarly, an acidic pH favors the stabilization of microtubules by taxol (76). Thus, the acidic cytoplasmic pH of tumor cells increases the activity of chemotherapeutic drugs. The more neutral pH of nontransformed and MDR cells decreases their activity.

In the PSS model, acidification of organelles plays a direct role in the accumulation of weak base chemotherapy agents. Still, it remains to be determined whether the drugs are actually exocytosed from the cell, and whether acidification may subserve other functions in pathways of cellular detoxification. Further, we do not know if sequestering chemotherapeutic drugs within subcellular organelles followed by secretion is sufficient to account for all the drug

resistance of MCF-7/ADR cells. However, based on the observation that disrupting organellar acidification in drug-resistant MCF-7/ADR cells (with either the protonophore monensin or H^+-ATPase blockers bafilomycin A1 and concanamycin A) both reverses the subcellular Adriamycin distribution to that seen in drug-sensitive MCF-7 cells (Figs. 7 and 8) and increases Adriamycin toxicity (21), we propose that the organelles make a significant contribution to the drug-resistance phenotype.

References

1. Biedler, J.L., and H. Riehm. 1970. Cellular resistance to actinomycin D in Chinese hamster cells in vitro: cross-resistance, radioautographic, and cytogenetic studies. *Cancer Res.* 30:1174–1184.
2. Simon, S.M., and M. Schindler. 1994. Cell biological mechanisms of multidrug resistance in tumors. *Proc. Natl. Acad. Sci. USA* 91:3497–3504.
3. Ling, V. 1975. Drug resistance and membrane alteration in mutants of mammalian cells. *Can. J. Genet. Cytol.* 17:503–515.
4. Gottesman, M.M., and I. Pastan. 1993. Biochemistry of multidrug resistance mediated by the multidrug transporter. *Annu. Rev. Biochem.* 62:385–427.
5. Cole, S.P.C., G. Bhardwaj, J.H. Gerlach, J.E. Mackie, C.E. Grant, K.C. Almquist, A.J. Stewart, E.U. Kurz, A.M.V. Duncan, and R.G. Deeley. 1992. Overexpression of a transporter gene in a multidrug-resistant human lung cancer cell line. *Science.* 258:1650–1654.
6. De la Torre, M., X.-Y. Hao, R. Larsson, P. Nygren, T. Tsuruo, B. Mannervik, and J. Bergh. 1993. Characterization of four doxorubicin adapted human breast cancer cell lines with respect to chemotherapeutic drug sensitivity, drug resistance associated membrane proteins and glutathione transferases. *Anticancer Res.* 13:1425–1430.
7. Posada, J.A., E.M. McKeegan, K.F. Worthington, M.J. Morin, S. Jaken, and T.R. Tritton. 1989. Human multidrug resistant KB cells overexpress protein kinase C: involvement in drug resistance. *Cancer Commun.* 1:285–292.
8. Beck, W.T. 1990. Mechanisms of multidrug resistance in human tumor cells. The roles of P-glycoprotein, DNA topoisomerase II, and other factors. *Cancer Treat. Rev.* 17(Suppl. A):11–20.
9. Ma, L., and M.S. Center. 1992. The gene encoding vacuolar H(+)-ATPase subunit C is overexpressed in multidrug-resistant HL60 cells. *Biochem. Biophys. Res. Commun.* 182:675–681.
10. Hindenburg, A.A., J.E. Gervasoni, Jr., S. Krishna, V.J. Stewart, M.L.J. Rosado, K. Bhalla, M.A. Baker, and R.N. Taub. 1989. Intracellular distribution and pharmacokinetics of daunorubicin in anthracycline-sensitive and -resistant HL-60 cells. *Cancer Res.* 49:4607–4614.
11. Gervasoni, J.E., Jr., S.Z. Fields, S. Krishna, M.A. Baker, M. Rosado, K. Thuraisamy, A.A. Hindenburg, and R.N. Taub. 1991. Subcellular distribution of daunorubicin in P-glycoprotein-positive and -negative drug-resistant cells using laser-assisted confocal microscopy. *Cancer Res.* 51:4955–4963.
12. Weaver, J.L., P.S. Pine, A. Aszalos, P.V. Schoenlein, S.J. Currier, R. Padmanabhan, and M.M. Gottesman. 1991. Laser scanning and confocal microscopy of daunorubicin, doxorubicin, and rhodamine 123 in multidrug-resistant cells. *Exp. Cell Res.* 196:323–329.
13. Coley, H.M., W.B. Amos, P.R. Twentyman, and P. Workman. 1993. Examination by laser scanning confocal fluorescence imaging microscopy of the subcellular localisation of anthracyclines in parent and multidrug resistant cell lines. *Br. J. Cancer.* 67:1316–1323.
14. Rutherford, A.V., and M.C. Willingham. 1993. Ultrastructural localization of daunomycin in multidrug-resistant cultured cells with modulation of the multidrug transporter. *J. Histochem. Cytochem.* 41:1573–1577.
15. Burns, J.H. 1972. *Anal. Profiles Drug Subst.* 1:463–480.
16. Beijnen, J.H. 1988. *Anal. Profiles Drug Subst.* 17:221–258.
17. Mayer, L.D., M.B. Bally, and P.R. Cullis. 1986. Uptake of adriamycin into large unilamellar vesicles in response to a pH gradient. *Biochim. Biophys. Acta* 857:123–126.
18. Dalmark, M., and H.H. Storm. 1981. A Fickian diffusion transport process with features of transport catalysis. Doxorubicin transport in human red blood cells. *J. Gen. Physiol.* 78:349–364.
19. Dalmark, M., and E.K. Hoffmann. 1983. Doxorubicin (Adriamycin) transport in Ehrlich ascites tumour cells: comparison with transport in human red blood cells. *Scand. J. Clin. Lab. Invest.* 43:241–248.
20. Beck, W.T. 1987. The cell biology of multiple drug resistance. *Biochem. Pharmacol.* 36:2879–2887.
21. Schindler, M., S. Grabski, E. Hoff, and S.M. Simon. 1996. Defective pH regulation of acidic compartments in human breast cancer cells (MCF-7) is normalized in adriamycin-resistant cells (MCF-7adr). *Biochemistry.* 35:2811–2817.
22. Keizer, H.G., and H. Joenje. 1989. Increased cytosolic pH in multidrug-resistant human lung tumor cells: effect of verapamil. *J. Natl. Cancer Inst.* 81:706–709.
23. Thiebaut, F., S.J. Currier, J. Whitaker, R.P. Haugland, M.M. Gottesman, I. Pastan, and M.C. Willingham. 1990. Activity

of the multidrug transporter results in alkalinization of the cytosol: measurement of cytosolic pH by microinjection of a pH-sensitive dye. *J. Histochem. Cytochem.* 38:685–690.

24. Hoffman, M.M., L.Y. Wei, and P.D. Roepe. 1996. Are altered pHi and membrane potential in hu MDR 1 transfectants sufficient to cause MDR protein-mediated multidrug resistance? *J. Gen. Physiol.* 108:295–313.

25. Simon, S.M., D. Roy, and M. Schindler. 1994. Intracellular pH and the control of multidrug resistance. *Proc. Natl. Acad. Sci. USA.* 91:1128–1132.

26. Millot, C., J.M. Millot, H. Morjani, A. Desplaces, and M. Manfait. 1997. Characterization of acidic vesicles in multidrug-resistant and sensitive cancer cells by acridine orange staining and confocal microspectrofluorometry. *J. Histochem. Cytochem.* 45:1255–1264.

27. Tycko, B., and F.R. Maxfield. 1982. Rapid acidification of endocytic vesicles containing α2-macroglobulin. *Cell.* 28:643–651.

28. Yamashiro, D.J., and F.R. Maxfield. 1987. Acidification of morphologically distinct endosomes in mutant and wild-type Chinese hamster ovary cells. *J. Cell Biol.* 105:2723–2733.

29. Augenbraun, E., F.R. Maxfield, R. St. Jules, W. Setlik, and E. Holtzman. 1993. Properties of acidified compartments in hippocampal neurons. *Eur. J. Cell Biol.* 61:34–43.

30. Pagano, R.E., O.C. Martin, H.C. Kang, and R.P. Haugland. 1991. A novel fluorescent ceramide analogue for studying membrane traffic in animal cells: accumulation at the Golgi apparatus results in altered spectral properties of the sphingolipid precursor. *J. Cell Biol.* 113:1267–1279.

31. Ghosh, R.N., and F.R. Maxfield. 1995. Evidence for non-vectorial, retrograde transferrin trafficking in the early endosomes of HEp2 cells. *J. Cell Biol.* 128:549–561.

32. Schmid, S., R. Fuchs, M. Kielian, A. Helenius, and I. Mellman. 1989. Acidification of endosome subpopulations in wild-type Chinese hamster ovary cells and temperature-sensitive acidification-defective mutants. *J. Cell Biol.* 108:1291–1300.

33. Lukacs, G.L., O.D. Rotstein, and S. Grinstein. 1990. Phagosomal acidification is mediated by a vacuolar-type H(+)-ATPase in murine macrophages. *J. Biol.Chem.* 265:21099–21107.

34. McNeil, P.L., R.F. Murphy, F. Lanni, and D.L. Taylor. 1984. A method for incorporating macromolecules into adherent cells. *J. Cell Biol.* 98:1556–1564.

35. Hoock, T.C., L.L. Peters, and S.E. Lux. 1997. Isoforms of ankyrin-3 that lack the NH$_2$-terminal repeats associate with mouse macrophage lysosomes. *J. Cell Biol.* 136:1059–1070.

36. Vickers, P.J., R.B. Dickson, R. Shoemaker, and K.H. Cowan. 1988. A multidrug-resistant MCF-7 human breast cancer cell line which exhibits cross-resistance to antiestrogens and hormone-independent tumor growth in vivo. *Mol. Endocrinol.* 2:886–892.

37. Rabkin, S.W., and P. Sunga. 1987. The effect of doxorubicin (adriamycin) on cytoplasmic microtubule system in cardiac cells. *J. Mol. Cell. Cardiol.* 19:1073–1083.

38. Zunino, F., R. Gambetta, A. Di Marco, A. Velcich, A. Zaccara, F. Quadrifoglio, and V. Crescenzi. 1977. The interaction of adriamycin and its beta anomer with DNA. *Biochim. Biophys. Acta.* 476:38–46.

39. Harris, A.L., and D. Hochhauser. 1992. Mechanisms of multidrug resistance in cancer treatment. *Acta Oncol.* 31:205–213.

40. Glickman, J., K. Croen, S. Kelly, and Q. Al-Awqati. 1983. Golgi membranes contain an electrogenic H$^+$ pump in parallel to a chloride conductance. *J. Cell Biol.* 97:1303–1308.

41. Mellman, I., R. Fuchs, and A. Helenius. 1986. Acidification of the endocytic and exocytic pathways. *Annu. Rev. Biochem.* 55:663–700.

42. Kim, J.H., C.A. Lingwood, D.B. Williams, W. Furuya, M.F. Manolson, and S. Grinstein. 1996. Dynamic measurement of the pH of the Golgi complex in living cells using retrograde transport of the verotoxin receptor. *J. Cell Biol.* 134:1387–1399.

43. Presley, J.F., S. Mayor, K.W. Dunn, L.S. Johnson, T.E. McGraw, and F.R. Maxfield. 1993. The End2 mutation in CHO cells slows the exit of transferrin receptors from the recycling compartment but bulk membrane recycling is unaffected. *J. Cell Biol.* 122:1231–1241.

44. McGraw, T.E., K.W. Dunn, and F.R. Maxfield. 1993. Isolation of a temperature-sensitive variant Chinese hamster ovary cell line with a morphologically altered endocytic recycling compartment. *J. Cell Physiol.* 155:579–594.

45. Lipsky, N.G., and R.E. Pagano. 1985. A vital stain for the Golgi apparatus. *Science.* 228:745–747.

46. Chen, J.W., T.L. Murphy, M.C. Willingham, I. Pastan, and J.T. August. 1985. Identification of two lysosomal membrane glycoproteins. *J. Cell Biol.* 101:85–95.

47. Vigevani, A., and M.J. Williamson. 1980. *Anal. Profiles Drug Subst.* 9:245–274.

48. Mayer, L.D., L.C.L. Tai, M.B. Bally, G.N. Mitilenes, R.S. Ginsberg, and P.R. Cullis. 1990. Characterization of liposomal systems containing doxorubicin entrapped in response to pH gradients. *Biochim. Biophys. Acta* 1025:143–151.

49. Barasch, J., M.D. Gershon, E.A. Nunez, H. Tamir, and Q. Al-Awqati. 1988. Thyrotropin induces the acidification of the secretory granules of parafollicular cells by increasing the chloride conductance of the granular membrane. *J. Cell Biol.* 107:2137–2147.

50. Zelenin, A.V. 1993. Acridine orange as a probe for molecular and cell biology. *In* Fluorescent and Luminescent Probes for Biological Activity. W.T. Mason, editor. Academic Press, Inc., San Diego. 83–99.

51. Berglindh, T., D.R. Dibona, S. Ito, and G. Sachs. 1980. Probes of parietal cell function. *Am. J. Physiol.* 238:G165–G176.

52. Allen, R.D., and A.K. Fok. 1983. Nonlysosomal vesicles (acidosomes) are involved in phagosome acidification in Paramecium. *J. Cell Biol.* 97:566–570.

53. Kreis, T.E., R. Matteoni, M. Hollinshead, and J. Tooze. 1989. Secretory granules and endosomes show saltatory movement biased to the anterograde and retrograde directions, respectively, along microtubules in AtT20 cells. *Eur. J. Cell Biol.* 49:128–139.

54. Fagotto, F., and F.R. Maxfield. 1994. Changes in yolk platelet pH during *Xenopus laevis* development correlate with yolk utilization. A quantitative confocal microscopy study. *J. Cell Sci.* 107:3325–3337.

55. Soule, H.D., T.M. Maloney, S.R. Wolman, W.D.J. Peterson, R. Brenz, C.M. McGrath, J. Russo, R.J. Pauley, R.F. Jones, and S.C. Brooks. 1990. Isolation and characterization of a spontaneously immortalized human breast epithelial cell line, MCF-10. *Cancer Res.* 50:6075–6086.

56. Murphy, R.F., S. Powers, and C.R. Cantor. 1984. Endosome pH measured in single cells by dual fluorescence flow cytometry: rapid acidification of insulin to pH 6. *J. Cell Biol.* 98:1757–1762.

57. Boscoboinik, D., R.S. Gupta, and R.M. Epand. 1990. Investigation of the relationship between altered intracellular pH

and multidrug resistance in mammalian cells. *Br. J. Cancer.* 61:568–572.

58. Di Virgilio, F., T.H. Steinberg, and S.C. Silverstein. 1990. Inhibition of Fura-2 sequestration and secretion with organic anion transport blockers. *Cell Calcium.* 11:57–62.

59. Homolya, L., Z. Holló, U.A. Germann, I. Pastan, M.M. Gottesman, and B. Sarkadi. 1993. Fluorescent cellular indicators are extruded by the multidrug resistance protein. *J. Biol. Chem.* 268:21493–21496.

60. Seksek, O., and J. Bolard. 1996. Nuclear pH gradient in mammalian cells revealed by laser microspectrofluorimetry. *J. Cell Sci.* 109:257–262.

61. Tartakoff, A.M., and P. Vassalli. 1978. Comparative studies of intracellular transport of secretory proteins. *J. Cell Biol.* 79: 694–707.

62. Maxfield, F.R. 1982. Weak bases and ionophores rapidly and reversibly raise the pH of endocytic vesicles in cultured mouse fibroblasts. *J. Cell Biol.* 95:676–681.

63. Dröse, S., and K. Altendorf. 1997. Bafilomycins and concanamycins as inhibitors of V-ATPases and P-ATPases. *J. Exp. Biol.* 200:1–8.

64. Feldherr, C.M., E. Kallenbach, and N. Schultz. 1984. Movement of a karyophilic protein through the nuclear pores of oocytes. *J. Cell Biol.* 99:2216–2222.

65. Barasch, J., B. Kiss, A. Prince, L. Saiman, D. Gruenert, and Q. Al-Awqati. 1991. Defective acidification of intracellular organelles in cystic fibrosis. *Nature.* 352:70–73.

66. Al-Awqati, Q., J. Barasch, and D.W. Landry. 1989. Proton pumps and chloride channels in secretory vesicles. *Soc. Gen. Physiol. Ser.* 44:283–294.

67. Baldini, N., K. Scotlandi, M. Serra, T. Shikita, N. Zini, A. Ognibene, S. Santi, R. Ferracini, and N.M. Maraldi. 1995. Nuclear immunolocalization of P-glycoprotein in multidrug-resistant cell lines showing similar mechanisms of doxorubicin distribution. *Eur. J. Cell Biol.* 68:226–239.

68. Molinari, A., M. Cianfriglia, S. Meschini, A. Calcabrini, and G. Arancia. 1994. P-glycoprotein expression in the Golgi apparatus of multidrug-resistant cells. *Int. J. Cancer* 59:789–795.

69. Ehring, G.R., Y.V. Osipchuk, and M.D. Cahalan. 1994. Swelling-activated chloride channels in multidrug-sensitive and -resistant cells. *J. Gen. Physiol.* 104:1129–1161.

70. Gill, D.R., S.C. Hyde, C.F. Higgins, M.A. Valverde, G.M. Mintenig, and F.V. Sepúlveda. 1992. Separation of drug transport and chloride channel functions of the human multidrug resistance P-glycoprotein. *Cell.* 71:23–32.

71. Hainsworth, A.H., R.M. Henderson, M.E. Hickman, S.B. Hladky, T. Rowlands, P.R. Twentyman, and M.A. Barrand. 1996. Hypotonicity-induced anion fluxes in cells expressing the multidrug-resistance-associated protein, MRP. *Pflugers Archiv.—Eur. J. Physiol.* 432:234–240.

72. Hardy, S.P., H.R. Goodfellow, M.A. Valverde, D.R. Gill, F.V. Sepúlveda, and C.F. Higgins. 1995. Protein kinase C-mediated phosphorylation of the human multidrug resistance P-glycoprotein regulates cell volume-activated chloride channels. *EMBO (Eur. Mol. Biol. Organ.) J.* 14:68–75.

73. Valverde, M.A., M. Díaz, F.V. Sepúlveda, D.R. Gill, S.C. Hyde, and C.F. Higgins. 1992. Volume-regulated chloride channels associated with the human multidrug-resistance P-glycoprotein. *Nature.* 355:830–833.

74. Dong, Y., G. Chen, G.E. Durán, K. Kouyama, A.C. Chao, B.I. Sikic, S.V. Gollapudi, S. Gupta, and P. Gardner. 1994. Volume-activated chloride current is not related to P-glycoprotein overexpression. *Cancer Res.* 54:5029–5032.

75. Mukhopadhyay, K., P.K. Parrack, and B. Bhattacharyya. 1990. The carboxy terminus of the alpha subunit of tubulin regulates its interaction with colchicine. *Biochemistry.* 29:6845–6850.

76. Ringel, I., and S.B. Horwitz. 1991. Effect of alkaline pH on taxol-microtubule interactions. *J. Pharmacol. Exp. Ther.* 259: 855–860.